Three-Dimensional Model for the Membrane Domain of *Escherichia coli* Leader Peptidase Based on Disulfide Mapping†

Paul Whitley, Lennart Nilsson, and Gunnar von Heijne*

Karolinska Institute Center for Structural Biochemistry, NOVUM, S-141 57 Huddinge, Sweden

Received December 29, 1992; Revised Manuscript Received June 1, 1993

ABSTRACT: We have mapped the interface between the two transmembrane α-helices in the membrane domain of the *Escherichia coli* enzyme leader peptidase by analyzing disulfides formed between pairs of cysteine residues introduced near their respective periplasmic ends. The interface is formed primarily from aliphatic amino acids, and the two helices appear to pack against each other in a left-handed supercoil. We suggest that disulfide mapping may be a generally applicable approach for the construction of models of helix–helix interfaces in membrane proteins.

So far as is known, there are two basic structural families of integral membrane proteins: the hydrophobic helix bundle proteins as exemplified by the photosynthetic reaction center complex (Deisenhofer & Michel, 1991), the light-harvesting chlorophyll a/b protein (Kühlbrandt & Wang, 1991), and bacteriorhodopsin (Henderson et al., 1990), and the hydrophobic β-barrel proteins as exemplified by the bacterial outer membrane porins (Weiss et al., 1991; Welte et al., 1991; Cowan et al., 1992). In this paper, we focus on the helix bundle proteins, where the membrane-embedded domain is formed by hydrophobic transmembrane α-helices (Rees et al., 1989). The orientation of this class of membrane proteins in the bilayer is determined largely by the distribution of positively charged amino acids in regions flanking the transmembrane segments—the "positive inside" rule (von Heijne & Gavel, 1988)—and can indeed be manipulated by the addition or removal of such residues in critical locations (Boyd & Beckwith, 1990; von Heijne & Manoil, 1990). The approximate positions of transmembrane helices in the protein sequence can generally be quite well predicted from hydrophobicity plots in conjunction with an analysis of the distribution of positively charged amino acids in candidate structures (von Heijne, 1992; Sipos & von Heijne, 1993) and can also be experimentally determined by a number of techniques (Jennings, 1989).

To go beyond this kind of secondary structure analysis toward full 3D structure models, experimental and theoretical methods that allow a more or less precise determination of helix–helix interfaces in a helix bundle must be developed. Ideally, high-resolution methods such as X-ray crystallography, electron microscopy, or NMR would provide this kind of data, but these have so far been difficult to apply to membrane proteins. It is thus important to explore alternatives based on genetic engineering and molecular modeling that might be used to construct 3D models of helix–helix interactions and to study the structural role of individual residues in the helix–helix interface.

To this end, we have made an initial study of leader peptidase (Lep), an enzyme from the inner membrane of *Escherichia coli* that removes signal peptides from secretory proteins. Lep has two transmembrane segments, H1 and H2, and is oriented with both the N-terminus and a large C-terminal domain (P2) in the periplasm (Wolfe et al., 1983; Moore & Miura, 1987; Lee et al., 1992b) (Figure 1). To map the interface between the H1 and H2 segments, we have introduced cysteine residues in various positions near their respective periplasmic ends and have assayed for the formation of disulfide bonds in a total of 19 double-Cys mutants. The pattern of Cys–Cys pairs that form disulfides has then been used as a basis for further modeling of the 3D structure of the H1–H2 membrane-embedded domain. A similar approach to the mapping of the transmembrane domain of the *E. coli* Tar receptor was reported recently (Pakula & Simon, 1992).

MATERIAL AND METHODS

Enzymes and Chemicals. Trypsin, soybean trypsin inhibitor, chicken egg white lysozyme, iodoacetamide, dithiothreitol (DTT), and phenylmethanesulfonyl fluoride were from Sigma. All DNA-modifying enzymes were from Promega and Pharmacia (T7 DNA polymerase).

Strains and Plasmids. Leader peptidase mutants were expressed from the pING1 plasmid (Johnston et al., 1985) in *E. coli* strain MC1061 (Δ*lacX74 araD139* Δ(*ara, leu*)*7697, galU, galK, hsr, hsm, strA*) (Dalbey & Wickner, 1986).

DNA Techniques. Site-specific mutagenesis was performed according to the method of Kunkel (1985), as modified by Geisselsoder et al. (1987). All mutants were confirmed by DNA sequencing of single-stranded M13 DNA using T7 DNA polymerase. Cloning into the pING1 plasmid was performed as described (Dalbey & Wickner, 1987).

Assays for Disulfide Bond Formation. Two assays for disulfide bond formation were used. In the first, cells were grown overnight at 37 °C in M9 minimal medium supplemented with ampicillin (100 μg/mL), 0.5% fructose, and all amino acids except methionine were back-diluted into the same medium (25 μL of cells into 0.5 mL of medium) and grown for an additional 3.5–4 h at 37 °C. Expression of the mutant leader peptidase constructs was induced by addition of arabinose (0.2% final concentration) and incubation for 5 min. Cells were then labeled with 30 μCi of [^{35}S]Met for 2 min, transferred to microcentrifuge tubes containing 50 μL of ice-cold 200 mM iodoacetamide (20 mM final concentration), and incubated on ice for 10 min to block all free sulfhydryls. Samples were precipitated by addition of trichloroacetic acid (10% final concentration), washed with

† This work was supported by grants from the Swedish Natural Sciences Research Council (NFR), the Swedish Technical Research Council (TFR), and the Swedish National Board for Industrial and Technical Development (NUTEK) to G.v.H.

* To whom correspondence should be addressed.

0006-2960/93/0432-8534$04.00/0

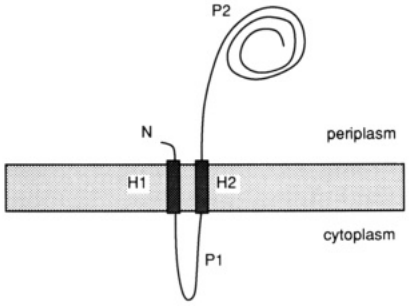

H1: M_1ANMFALILVIATLVTGILWSVDK...

H2: ...G_{58}WLETGASVFPVLAIVLIVRSFIYEP...

FIGURE 1: Orientation of Lep in the inner membrane of *E. coli*. The two hydrophobic transmembrane segments H1 and H2 are indicated, together with the cytoplasmic and periplasmic domains P1 and P2. Also shown are the amino acid sequences of H1 and H2, with the positions of the cysteine mutations indicated by an asterisk (*). R_{77} in H2 was not mutated, since this would probably affect the position of H2 in the membrane (c.f., Bilgin et al., 1990). Note that residue 21 in H1 is a cysteine in the wild-type sequence but has been changed to serine in all Cys–Cys double mutants.

acetone, resuspended in 10 mM Tris–2% SDS, and immunoprecipitated with Lep antiserum. Half of each sample was resuspended in sample buffer containing 50 mM DTT, and the remainder in sample buffer lacking DTT. Samples were heated to 70 °C for 5 min before analysis by SDS–PAGE (10% separating gel) and autoradiography.

In the second assay, cells were grown as above, and the culture was split in two just before induction with arabinose. One sample was treated as above; to the other, iodoacetamide (20 mM final concentration) was added 30 s before the [^{35}S]-Met labeling in order to prevent disulfide bond formation. After work-up, both samples were analyzed by SDS–PAGE in sample buffer not containing DTT.

Molecular Modeling. For the 3D modeling study, two segments roughly corresponding to transmembrane helices H1 and H2 were used. An initial model was constructed from two ideal α-helices comprising residues 1–18 (H1) and 65–82 (H2) which were manually docked using interactive molecular graphics (QUANTA, Molecular Simulations Inc., Waltham, MA) so that the residues capable of forming disulfide bridges on H1 were close to their counterparts on H2.

This initial model was energy minimized (500 steps of steepest descent minimization) without any restraints, prior to the refinement cycles using energy minimization and molecular dynamics simulation protocols incorporating the experimental data in the form of constraints on the S–S distances between residue pairs known to form disulfides. The restraints were added to the standard potential energy function according to

$$E_{S\text{-}S} = 0.5k_{S\text{-}S}(r_{S\text{-}S} - r_{ref})^2; \quad r_{S\text{-}S} > r_{ref}$$

where the reference distance r_{ref} was set to 2 Å, and $r_{S\text{-}S}$ is the S–S distance between two cysteine residues that form a disulfide. Finally, a nonrestrained energy minimization was carried out after replacing the six nonnative cysteines with their corresponding wild-type residues.

All calculations were performed with the program CHARMM (Brooks et al., 1983) using parameter set par all22 prot b3 (M. Karplus, personal communication) *in vacuo*. Electrostatic interactions were shifted to zero at a cut-off distance of 12 Å. Minimizations were performed with steepest descent and Adopted-Basis Newton Raphson (ABNR) algorithms (Brooks et al., 1983), and in the MD simulations the standard Verlet algorithm was used (Verlet, 1967). Restrained minimizations were performed in two stages of 500 steps of ABNR minimization, with the force constant $k_{S\text{-}S}$ set to 5 and 25 kcal/(mol·Å^2), respectively.

Table I: Cys–Cys Mutants and C_β–C_β Distances for the Corresponding Wild-Type Side Chains in the Final Model

mutant	C_β–C_β distance (Å)	disulfide
C_2,C_{75}	10.8	no
C_3,C_{75}	5.4	yes
C_4,C_{75}	7.6	yes
C_5,C_{75}	11.4	no
C_2,C_{76}	12.7	no
C_3,C_{76}	8.0	possible[a]
C_4,C_{76}	6.3	yes
C_5,C_6	11.9	no
C_2,C_{78}	9.7	no
C_3,C_{78}	5.2	no
C_4,C_{78}	8.8	no
C_5,C_{78}	12.3	no
C_2,C_{79}	8.4	no
C_3,C_{79}	5.1	possible[a]
C_4,C_{79}	4.7	yes
C_5,C_{79}	9.1	no
C_8,C_{75}	11.3	no
C_7,C_{75}	5.7	yes
C_8,C_{79}	11.3	no

[a] These mutants have a fuzzy appearance in nonreducing gels and were not used in the restrained energy minimizations.

RESULTS

Disulfide Mapping of the H1–H2 Interface. A catalytically active Lep mutant where the three cysteines present in the wild-type protein (residues 21, 170, and 176) have all been changed to serine (Sung & Dalbey, 1992) was used as a starting point for the study. This was necessary, as a disulfide is formed between Cys_{170} and Cys_{176} in the wild-type protein (our unpublished data). A number of residues near the N-terminus of the H1 transmembrane segment were individually changed to cysteine, and, starting from these single-cysteine mutants, a second cysteine was introduced in a number of positions near the C-terminus of the H2 transmembrane segment (Figure 1). All double-Cys mutants inserted into the inner membrane in the same orientation as wild-type Lep [as determined by protease-mapping (von Heijne, 1989), data not shown] and all were found to have wild-type catalytic activity in a sensitive *in vivo* assay (Bilgin et al., 1990), except for all single- and double-Cys mutants where Asn_3 had been changed to Cys. Apparently, a cysteine in this particular position compromises the catalytic activity of Lep without affecting its membrane assembly properties (our unpublished data).

Nineteen double-Cys mutants were made in all (Table I). To assay for disulfide formation, the mutant proteins were expressed and radiolabeled by [^{35}S]Met *in vivo*. Iodoacetamide was then added to modify all free cysteines and to prevent the formation of disulfides during further work-up; cells were TCA-precipitated, resuspended, immunoprecipitated with Lep antiserum, and analyzed by SDS–PAGE under both reducing and nonreducing conditions. Disulfide formation between any H1- and H2-cysteines should be apparent as an increased mobility in the nonreducing compared to the reducing gel. A second assay was also used, where half of the culture was

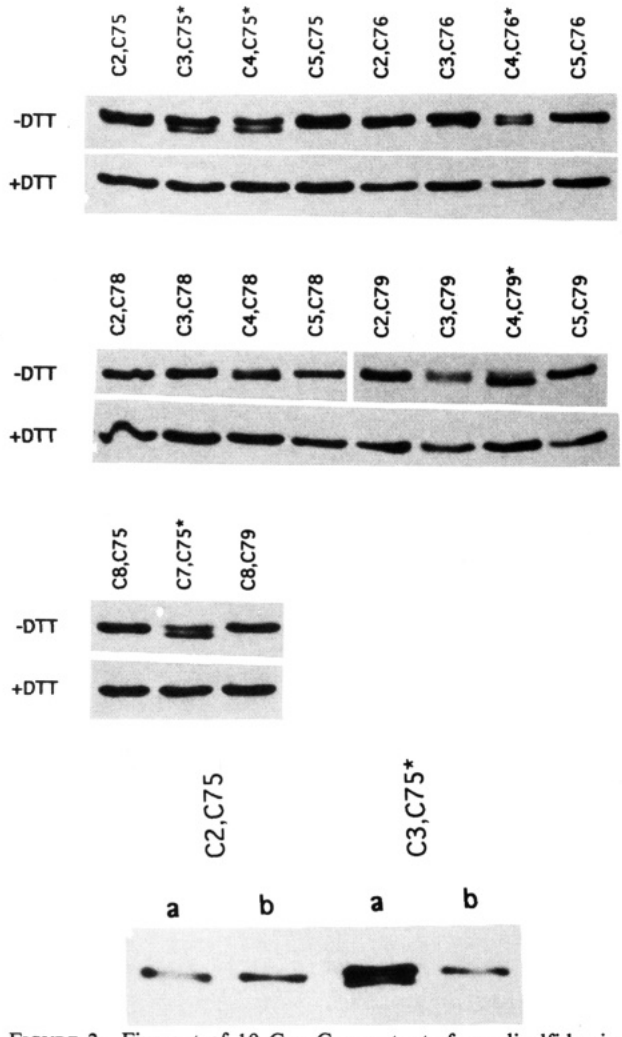

FIGURE 2: Five out of 19 Cys–Cys mutants form disulfides in a nonreducing environment. (a, top) Synthesis of Lep mutants was induced by arabinose, cells were labeled with [^{35}S]Met for 2 min, and any free sulfhydryls were then covalently blocked with iodoacetamide. After immunoprecipitation with Lep antiserum, proteins were analyzed by both nonreducing (–DTT) and reducing (+DTT) SDS–PAGE and visualized by autoradiography. Formation of disulfides is seen as the appearance of a doublet band under nonreducing conditions (mutants marked *), with the faster-moving band representing the disulfide-bonded form. Note that the –DTT and +DTT data are from different gels; when run in the same gel, the reduced forms have the same mobilities as the upper bands in the –DTT lanes. (b, bottom) Results for two selected mutants when [^{35}S]Met labeling was performed either before (a lanes) or after (b lanes) addition of iodoacetamide (see Materials and Methods). In this case, SDS–PAGE was performed only under nonreducing conditions. Note that the results are very similar to those of panel a and that disulfide formation in the C3,C75 mutant is seen as a doublet in lane a.

treated with iodoacetamide for 30 s before labeling with [^{35}S]-Met to prevent all disulfide bond formation, whereas the other half was treated as above; one advantage of this second assay is that the samples treated with iodoacetamide before and after [^{35}S]Met labeling can both be run out in neighboring lanes on a nonreducing gel which makes it possible to detect smaller mobility shifts.

The results are shown in Figure 2. With the first assay (Figure 2a), most double-Cys mutants have the same mobility during reducing and nonreducing conditions, but five run as clear doublets in the nonreducing gel, indicating that a disulfide is formed in a significant fraction of these molecules. The five disulfides are formed between positions 3–75, 4–75, 4–76, 4–79, and 7–75; when plotted on a helical net diagram (Figure 3a), they define an interface that is consistent with H1 and H2 being α-helices and packed against each other in a typical left-handed supercoil with a *i,i+3/i,i+4* grooves-into-ridges pattern (Chothia et al., 1977). Two additional double-Cys mutants, C3,C76 and C3,C79 have a fuzzy appearance in the nonreducing gel, possibly suggesting the formation of a disulfide also in these cases; both disulfides would be compatible with the structure depicted in Figure 3. As exemplified in Figure 2b, identical results are obtained with the second assay; again the C3,C76 and C3,C79 mutants give a broad, fuzzy band when labeled in the absence but not in the presence of iodoacetamide (data not shown).

Modeling of the H1–H2 Interface Using Restrained Energy Minimization and Molecular Dynamics. A rough model structure of the H1–H2 domain, with Cys replacements at positions 3, 4, 7, 75, 76, and 79, was first refined by restrained energy minimizations. The restraints were applied either to just one single Cys–Cys pair at a time or simultaneously to the five pairs observed in Figure 2a.

During the restrained minimizations, stress induced by bad contacts introduced in the crude manual docking was relieved, and the residues capable of forming disulfides were brought closer together. The S–S distances were in all cases brought from 5–9 Å to below 3.2 Å (Table II), which is as close as these atoms can get in this system, with reduced cysteines. The overall helical structure of H1 and H2 remained intact, with a tendency of a kink showing around Pro_{68} in H2. Even though the refinements led to significant improvements in the Cys–Cys distances, there were no large alterations of the global structure, with root mean square atomic displacements from the initial model in the range 2–2.5 Å. The single-pair restrained minimizations showed a noticeable effect only on the restrained distance in each run. In all cases, the closest S–S distance was 3.1 Å, also when all five restraints were included, indicating that the set of five disulfides is internally consistent so that all can be formed, in the model, at the same time. Further refinement using molecular dynamics at a temperature of 600 K did not improve the fit to the experimental data (Table II) but rather caused structural deterioration, with substantial local disturbances of the helix structure at the C-terminal end of H2.

The final model was constructed starting from a structure obtained by taking the end result from the restrained minimization using all five restraints and, after replacing the six nonnative Cys residues with their corresponding wild-type residues, running a nonrestrained minimization. This final structure had no bad contacts, good secondary structure, and retained the residues of interest in close proximity. The angle between H1 and H2 was 12° (left-handed supercoil), compared to 6° in the initial model, so there had been a slight adjustment of the overall orientation of the helices, in addition to more local changes mainly influencing side chains. In the restrained minimizations, the structural changes are driven by the restraints, with only minor changes occurring in other parts of the structure. The presence of all six cysteines at the same time during the initial minimization has no major influence on the structure, as seen from the final model obtained with the native sequence.

Although more elaborate modeling schemes could be envisioned, we have opted for a minimalist approach consistent with the level of detail inherent in the experiment. Our model thus satisfies the experimental data, but we have not tried to explore possible structural variations around the proposed structure or to predict the structure by systematically analyzing all possible H1–H2 packings.

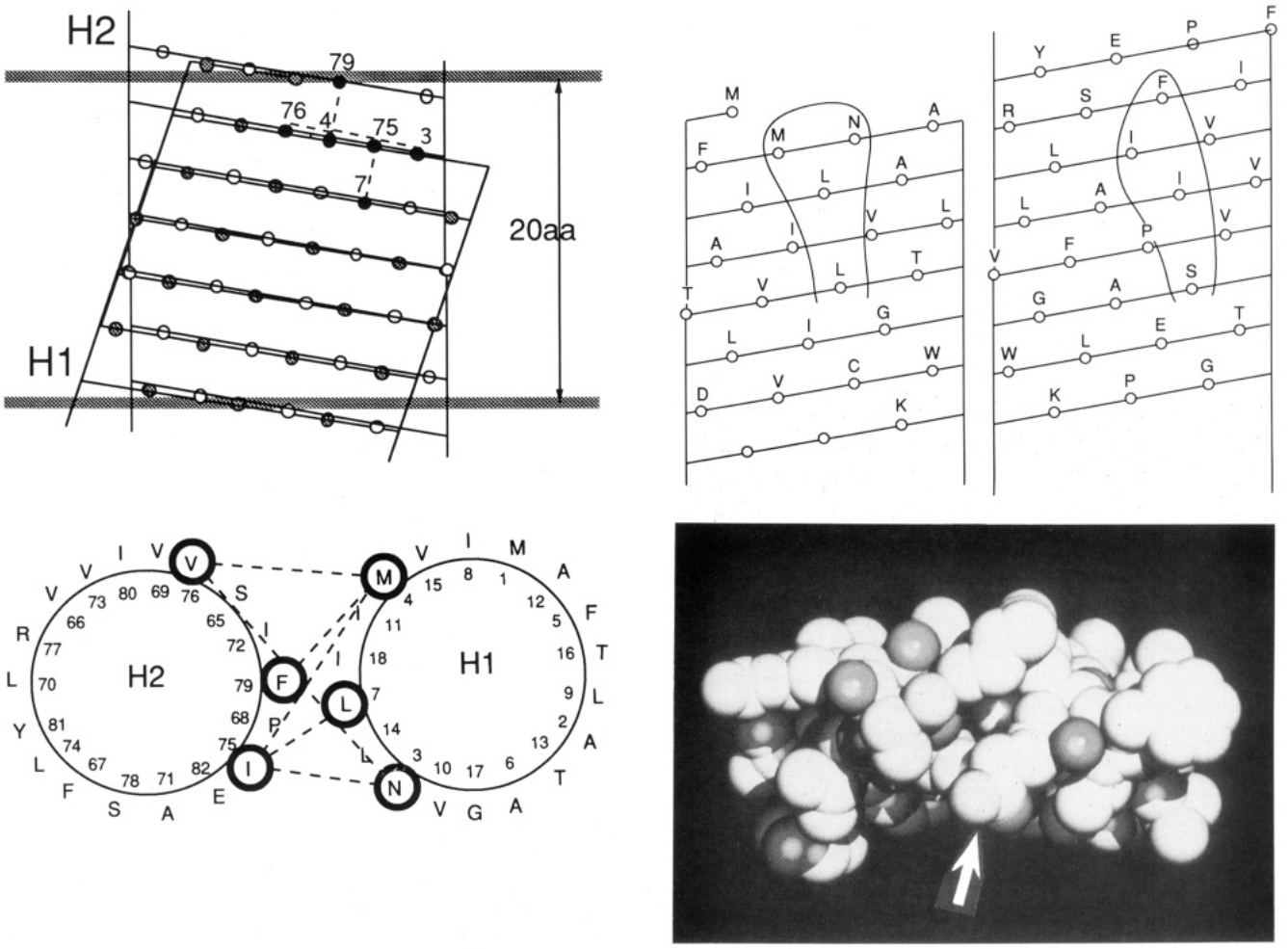

FIGURE 3: (a, top left) Helical net diagram of the H1–H2 interface with the disulfide bonds formed in the six Cys–Cys mutants marked. The relative orientation of H1 and H2 is that of a left-handed *i,i+3/i,i+4* grooves-into-ridges packing (H2 is shown on top of H1). The approximate position of the membrane is also indicated, with the cytoplasmic face downward. (b, top right) Residues with more than 50% of their surface area buried in the H1–H2 interface. Note that the model is more uncertain toward the cytoplasmic (bottom) end, where no accessibility pattern is shown. (c, bottom left) Helical wheel diagram with the six disulfide bonds marked (view from the periplasmic side). The signal peptide would be reaching up along the bottom face of the H1–H2 structure. (d, bottom right) Space-filling representation of the H1–H2 model. Asn_3 is indicated by an arrow. The orientation is the same as in panel c.

Table II: S–S Distances (Å) in Cysteine Pairs from Modeled Structures[a]

residue pair	init	all 5	RMD	3–75	4–75	4–76	4–79	7–75
3–75	6.1	3.1	3.4	3.1	3.8	3.7	3.7	4.2
4–75	9.5	3.2	4.2	8.9	3.1	7.6	8.3	8.3
4–76	6.9	3.1	3.5	7.1	5.5	3.1	7.5	8.6
4–79	5.3	3.2	3.2	5.2	4.1	5.3	3.1	4.6
7–75	4.4	3.2	3.6	4.4	4.2	3.9	4.4	3.2

[a] Structures used are as follows: init, the initial model; and RMD, the restrained MD end structure. The others are from restrained minimizations with all five restraints (all 5) or only one distance restraint (as indicated).

Solvent-accessible surface areas were calculated for the final model using a probe radius of 1.6 Å (Lee & Richards, 1971), both for the H1–H2 complex and for the two individual helices. The relative difference in accessible surface, averaged per residue, was calculated to characterize the degree to which each residue was involved in the contact surface between the two helices (Figure 3b).

DISCUSSION

By constructing a set of 19 double-cysteine mutants in the membrane-embedded domain of *E. coli* leader peptidase, five of which were found to make a disulfide bond, we have been able to approximately map the interface between the two transmembrane α-helices in the molecule. Other genetic techniques that have been used to map interfaces between transmembrane helices include mutational analysis of presumed functionally important residues (Collins et al., 1989), isolation of second-site revertants of nonfunctional mutant proteins (di Rago et al., 1990; Miller et al., 1990; Harris et al., 1991; King et al., 1991; Howitt & Cox, 1991; Lee et al., 1992a; Nelson & Douglas, 1992; Sahin-Tóth et al., 1992), and assays based on mutational perturbation of dimer formation between protein subunits (Manolios et al., 1990; Cosson et al., 1991; Cosson & Bonifacino, 1992; Lemmon et al., 1992; Rutledge et al., 1992). Compared to disulfide mapping, the major shortcoming of these other techniques is that they do not provide direct physical links between the two helices and hence do not provide very strong constraints for 3D modeling (except when the two helices are identical as in a homodimer). On the other hand, disulfide mapping requires that two residues in the interface are changed to cysteines, which may perturb the structure to an unknown extent. It is thus important to characterize a fairly large number of Cys–Cys mutants to obtain a consistent picture of the relative orientation of the two helices.

In our final model, the C_β–C_β distance for the residues that are close enough to make disulfides when replaced by cysteines

varies between 4.7 and 7.6 Å (Table I), and only minor structural adjustments (on the order of 1–3 Å) are necessary to bring the individual C_β–C_β distances to within the range found for naturally occurring disulfide bonds (<4.6 Å; Careaga & Falke, 1992). In fact, mutant C_4,C_{79}, which has the largest fraction of disulfide-bonded molecules of all the mutants (Figure 2), also has the shortest C_β–C_β distance (4.7 Å). Of the 12 Cys–Cys mutants that do not appear to form disulfides, only one (C_3,C_{78}) has a C_β–C_β distance similar to those found for the disulfide-forming mutants. The other 11 mutants have much longer C_β–C_β distances (8.8–12.7 Å) (Table I). Similar C_β–C_β distances for disulfide-forming Cys–Cys pairs were recently reported for a model of the two transmembrane helices in the *E. coli* Tar chemoreceptor based on disulfide mapping (Pakula & Simon, 1992), while much larger movements of secondary structure elements were in evidence in a study of engineered disulfides in the D-galactose chemosensory receptor, a globular *E. coli* protein of known 3D structure (Careaga & Falke, 1992).

In the Lep-model, eight residues lose 50% or more of their accessible surface area upon fomation of the H1–H2 interface (Figure 3): Asn_3, Met_4, Leu_7, Leu_{14}, Ser_{65}, Ile_{72}, Ile_{75}, and Phe_{79}. The interface is thus largely formed by hydrophobic amino acids and cannot be identified on the basis of helical amphiphilicity (not shown). This is similar to the recently mapped helical interfaces in the Tar chemoreceptor (Pakula & Simon, 1992), glycophorin A (Lemmon et al., 1992), and the MHC II α–β dimer (Cosson & Bonifacino, 1992), where the interface residues are mostly hydrophobic, but is in contrast to bacteriorhodopsin (Henderson et al., 1990) and the T-cell receptor oligomer (Cosson et al., 1991), where charged amino acids seem to reside in or even determine the interface region. This raises the interesting possibility that close-packing between hydrophobic residues may drive helix–helix association even in the nonpolar environment of a lipid bilayer (Efremov et al., 1992). We further note that Pro_{68} in H2, which is likely to introduce a kink in the helix, is largely buried in the interface (48% surface area lost upon formation of the interface), as expected from the tendency of prolines in known membrane protein structures to be shielded from the lipid environment (von Heijne, 1991). It is also noteworthy that, as in many other transmembrane segments (Martin et al., 1989; Cowan et al., 1992; Schiffer et al., 1992; Landolt-Marticorena et al., 1993), Trp and Tyr residues are found near the presumed positions of the phospholipid headgroups: thus, on the cytoplasmic side there are Trp_{20} and Trp_{59}, and Tyr_{81} on the periplasmic side (Figure 3b).

What, finally, does the H1–H2 structure tell us about the leader peptidase enzyme itself? Previous studies have shown that the membrane domain is largely irrelevant for function (Bilgin et al., 1990) and serves only as a membrane anchor; indeed, both the H1 and P1 regions are absent in the corresponding *Bacillus subtilis* enzyme, and the remaining transmembrane segment has no discernible homology to the H2 segment in *E. coli* Lep (van Dijl et al., 1992). On the other hand, since signal peptides span the inner membrane with their N-terminus tethered to the cytoplasmic side (Kuhn, 1987) and may be as short as 18 residues (von Heijne, 1985; von Heijne & Abrahmsén, 1989), the active site must be located close to the periplasmic membrane surface, i.e., presumably near the periplasmic ends of the H1 and H2 transmembrane segments. Further, Ser_{90}, which is only 14 residues downstream of H2, has been shown to be critical for function (Sung & Dalbey, 1992) and is in fact conserved in all known signal peptidases (Dalbey & von Heijne, 1992). This again suggests that the active site is close to the periplasmic ends of H1 and H2. Finally, as noted above, substitution of Asn_3 near the periplasmic end of H1 with Cys significantly affects the enzymatic activity, whereas the introduction of a number of other residues (Lys, Asp, Phe, Gln, Ser) in this position has no or only a weak effect (our unpublished data). The most straightforward interpretation is that Asn_3 is positioned sufficiently close to the active site that the introduction of a reactive –SH group in this location will result in a major detrimental effect on catalysis. If this is true, the signal peptide should reach up toward the active site along the center of the bottom face of the H1–H2 structure (Figure 3c,d) in a shallow depression defined by Ala_6, Val_{10}, and Leu_{14} on H1, and Pro_{68}, Ala_{71}, and Ile_{75} on H2. We note that this bottom face of the structure is considerably smoother than the upper face, which includes a number of bulky residues such as Ile_{11}, Val_{15}, Ile_{18}, Val_{69}, Ile_{72}, Val_{76}, and Phe_{79}, and thus possibly better fit to make contact with the hydrophobic part of the signal peptide.

ACKNOWLEDGMENT

Purified Lep used to produce Lep antiserum in rabbits was a gift from Dr. Bill Wickner, UCLA. Dr. Ross Dalbey, Ohio State University, kindly provided the Lep mutant lacking cysteines. Mark Kolkman, Annika Sääf, and IngMarie Nilsson provided expert technical assistance. Oligonucleotide synthesis was done by Zekiye Cansu at the Karolinska Institute Center for Biotechnology.

REFERENCES

Bilgin, N., Lee, J. I., Zhu, H., Dalbey, R., & von Heijne, G. (1990) *EMBO J. 9*, 2717.
Boyd, D., & Beckwith, J. (1990) *Cell 62*, 1031.
Brooks, B. R., Bruccoleri, R. E., Olafson, B. D., States, D. J., Swaminathan, S., & Karplus, M. (1983) *J. Comput. Chem. 4*, 187.
Careaga, C. L., & Falke, J. J. (1992) *J. Mol. Biol. 226*, 1219.
Chothia, C., Levitt, M., & Richardson, D. (1977) *Proc. Natl. Acad. Sci. U.S.A. 74*, 4130.
Collins, J. C., Permuth, S. F., & Brooker, R. J. (1989) *J. Biol. Chem. 264*, 14698.
Cosson, P., & Bonifacino, J. S. (1992) *Science 258*, 659.
Cosson, P., Lankford, S. P., Bonifacino, J. S., & Klausner, R. D. (1991) *Nature 351*, 414.
Cowan, S. W., Schirmer, T., Rummel, G., Steiert, M., Ghosh, R., Pauptit, R. A., Joansonius, J. N., & Rosenbusch, J. P. (1992) *Nature 358*, 727.
Dalbey, R. E., & Wickner, W. (1986) *J. Biol. Chem. 261*, 13844.
Dalbey, R. E., & Wickner, W. (1987) *Science 235*, 783.
Dalbey, R. E., & von Heijne, G. (1992) *Trends Biochem. Sci. 17*, 474.
Deisenhofer, J., & Michel, H. (1991) *Annu. Rev. Biophys. Biophys. Chem. 20*, 247.
di Rago, J. P., Netter, P., & Slonimski, P. P. (1990) *J. Biol. Chem. 265*, 15750.
Efremov, R. G., Gulyaev, D. I., & Modyanov, N. N. (1992) *J. Protein Chem. 11*, 699.
Geisselsoder, J., Witney, F., & Yuckenberg, P. (1987) *Bio-Techniques 5*, 786.
Harris, S. L., Perlin, D. S., Seto-Young, D., & Haber, J. E. (1991) *J. Biol. Chem. 266*, 24439.
Henderson, R., Baldwin, J. M., Ceska, T. A., Zemlin, F., Beckmann, E., & Downing, K. H. (1990) *J. Mol. Biol. 213*, 899.
Howitt, S. M., & Cox, G. B. (1992) *Proc. Natl. Acad. Sci. U.S.A. 89*, 9799.
Jennings, M. L. (1989) *Annu. Rev. Biochem. 58*, 999.
Johnston, S., Lee, J. H., & Ray, D. S. (1985) *Gene 34*, 137.

King, S. C., Hansen, C. L., & Wilson, T. H. (1991) *Biochim. Biophys. Acta 1062*, 177.
Kühlbrandt, W., & Wang, D. N. (1991) *Nature 350*, 130.
Kuhn, A. (1987) *Science 238*, 1413.
Kunkel, T. A. (1985) *Proc. Natl. Acad. Sci. U.S.A. 82*, 488.
Landolt-Marticorena, C., Williams, K. A., Deber, C. M., & Reithmeier, R. A. F. (1993) *J. Mol. Biol. 229*, 602.
Lee, B., & Richards, F. M. (1971) *J. Mol. Biol. 55*, 379.
Lee, J.-I., Hwang, P. P., Hansen, C., & Wilson, T. H. (1992a) *J. Biol. Chem. 267*, 20758.
Lee, J.-I., Kuhn, A., & Dalbey, R. E. (1992b) *J. Biol. Chem. 267*, 938.
Lemmon, M. A., Flanagan, J. M., Treutlein, H. R., Zhang, J., & Engelman, D. M. (1992) *Biochemistry 31*, 12719.
Manolios, N., Bonifacino, J. S., & Klausner, R. D. (1990) *Science 249*, 274.
Martin, A., Cheetham, J., & Rees, A. (1989) *Proc. Natl. Acad. Sci. U.S.A. 86*, 9268.
Miller, J. M., Oldenburg, M., & Fillingame, R. H. (1990) *Proc. Natl. Acad. Sci. U.S.A. 87*, 4900.
Moore, K. E., & Miura, S. (1987) *J. Biol. Chem. 262*, 8806.
Nelson, D. R., & Douglas, M. G. (1993) *J. Mol. Biol. 230*, 1171–1182.
Pakula, A. A., & Simon, M. I. (1992) *Proc. Natl. Acad. Sci. U.S.A. 89*, 4144.
Rees, D. C., Komiya, H., Yeates, T. O., Allen, J. P., & Feher, G. (1989) *Annu. Rev. Biochem. 58*, 607.
Rutledge, T., Cosson, P., Manolios, N., Bonifacino, J. S., & Klausner, R. D. (1992) *EMBO J. 11*, 3245.
Sahin-Tóth, M., Dunten, R. L., Gonzales, A., & Kaback, H. R. (1992) *Proc. Natl. Acad. Sci. U.S.A. 89*, 10547.
Schiffer, M., Chang, C. H., & Stevens, F. J. (1992) *Protein Eng. 5*, 213.
Sipos, L., & von Heijne, G. (1993) *Eur. J. Biochem. 213*, 1333.
Sung, M., & Dalbey, R. E. (1992) *J. Biol. Chem. 267*, 13154.
van Dijl, J. M., de Jong, A., Vehmaanperä, J., Venema, G., & Bron, S. (1992) *EMBO J. 11*, 2819.
Verlet, L. (1967) *Phys. Rev. 159*, 98.
von Heijne, G. (1985) *J. Mol. Biol. 184*, 99.
von Heijne, G. (1989) *Nature 341*, 456.
von Heijne, G. (1991) *J. Mol. Biol. 218*, 499.
von Heijne, G. (1992) *J. Mol. Biol. 225*, 487.
von Heijne, G., & Gavel, Y. (1988) *Eur. J. Biochem. 174*, 671.
von Heijne, G., & Abrahmsén, L. (1989) *FEBS Lett. 244*, 439.
von Heijne, G., & Manoil, C. (1990) *Protein Eng. 4*, 109.
Weiss, M. S., Kreusch, A., Schiltz, E., Nestel, U., Welte, W., Weckesser, J., & Schulz, G. E. (1991) *FEBS Lett. 280*, 379.
Welte, W., Weiss, M. S., Nestel, U., Weckesser, J., Schiltz, E., & Schulz, G. E. (1991) *Biochim. Biophys. Acta 1080*, 271.
Wolfe, P. B., Wickner, W., & Goodman, J. M. (1983) *J. Biol. Chem. 258*, 12073.